DESIGN, FABRICATION AND TESTING OF A PARABOLOIDAL REFLECTOR ANTENNA AND PULSER SYSTEM FOR IMPULSE-LIKE WAVEFORMS*

I.D. Smith and D.W. Morton
Pulse Sciences, Inc.
San Leandro, CA 94577

D.V. Giri and H. Lackner
Pro-Tech
Lafayette, CA 94545-3610

C.E. Baum and J.R. Marek
Phillips Laboratory
Kirtland AFB, NM 87117

Abstract

This paper describes the design and test of a radiating system for impulse-like waveforms. The antenna is a 3.66 meter diameter paraboloidal reflector fed by a pair of conical TEM feed structures. The pulse generator that feeds the TEM structures incorporates an electromagnetic lens to ensure a near-ideal spherical TEM wavelaunch, and a ≥ 120 kV, ~ 100 atm. hydrogen switch operating in burst mode at up to 200 Hz. The antenna radiates a waveform which is the time-derivative of the double exponential [~100 ps, 45 nsec 10-90% rise and fall] waveform supplied by the pulser.

Introduction

This paper describes a radiating system designed to produce an impulse-like waveform in the far field. The key elements of this system, shown in Figure 1 are: (I) a high-pressure hydrogen gas switch, (ii) an electromagnetic lens made of oil insulating medium, and (iii) a paraboloidal, non-dispersive antenna fed by

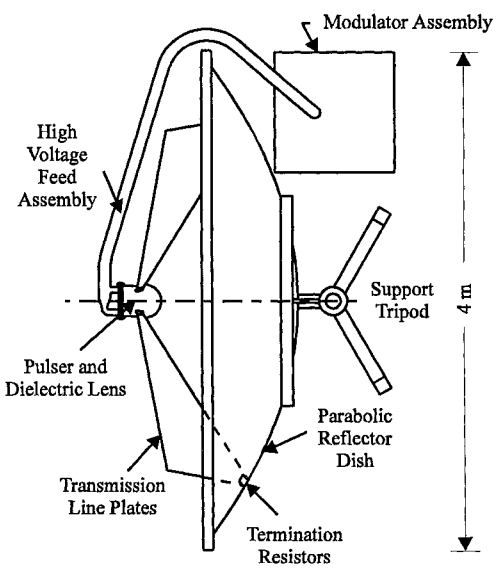

Figure 1. Top view of impulse radiation system (IRS).

This work was sponsored by Phillips Laboratory/WSR under Contract F29601-93-C-0185.

Report Documentation Page

Form Approved
OMB No. 0704-0188

1. REPORT DATE	2. REPORT TYPE	3. DATES COVERED
JUL 1995	**N/A**	**-**

4. TITLE AND SUBTITLE	5a. CONTRACT NUMBER
Design, Fabrication And Testing Of A Paraboloidal Reflector Antenna And Pulser System For Impulse-Like Waveforms	5b. GRANT NUMBER
	5c. PROGRAM ELEMENT NUMBER
6. AUTHOR(S)	5d. PROJECT NUMBER
	5e. TASK NUMBER
	5f. WORK UNIT NUMBER
7. PERFORMING ORGANIZATION NAME(S) AND ADDRESS(ES) **Pulse Sciences, Inc. San Leandro, CA 94577**	8. PERFORMING ORGANIZATION REPORT NUMBER
9. SPONSORING/MONITORING AGENCY NAME(S) AND ADDRESS(ES)	10. SPONSOR/MONITOR'S ACRONYM(S)
	11. SPONSOR/MONITOR'S REPORT NUMBER(S)

12. DISTRIBUTION/AVAILABILITY STATEMENT
Approved for public release, distribution unlimited

13. SUPPLEMENTARY NOTES
See also ADM002371. 2013 IEEE Pulsed Power Conference, Digest of Technical Papers 1976-2013, and Abstracts of the 2013 IEEE International Conference on Plasma Science. Held in San Francisco, CA on 16-21 June 2013. U.S. Government or Federal Purpose Rights License.

14. ABSTRACT
This paper describes the design and test of a radiating system for impulse-like waveforms. The antenna is a 3.66 meter diameter paraboloidal reflector fed by a pair of conical TEM feed structures. The pulse generator that feeds the TEM structures incorporates an electromagnetic lens to ensure a near-ideal spherical TEM wavelaunch, and a~ 120 kV,- 100 atm. hydrogen switch operating in burst mode at up to 200 Hz. The antenna radiates a waveform which is the time-derivative of the double exponential [-1 00 ps, 45 nsec 1 0-90% rise and fall] waveform supplied by the pulser.

15. SUBJECT TERMS

16. SECURITY CLASSIFICATION OF:			17. LIMITATION OF ABSTRACT	18. NUMBER OF PAGES	19a. NAME OF RESPONSIBLE PERSON
a. REPORT	b. ABSTRACT	c. THIS PAGE			
unclassified	**unclassified**	**unclassified**	**SAR**	**9**	

conical transmission lines. The hydrogen spark-gap switch results in a fast (10-90%) rise of <100 ps, while the electro-magnetic lens ensures a near-ideal spherical TEM wave launch. Because the launch is a TEM wave, the antenna is dispersionless. All of the frequencies contained in the input pulse travels at the same speed over the antenna and arrive at the same instant at a distant observer. This impulse radiating antenna (IRA) system produces a peak electric field of 4.2 kV/m and a FWHM $\simeq$130 ps at a distance of 304 meters from the antenna. Such an impulse-like far field has a very wide bandwidth (10's of MHz to a few GHz) and is expected to find many useful applications. The pulser produces a nearly double exponential waveform with an amplitude of 115-135 kV, <100 ps 10-90% rise, 20 nsec e-fold decay at a prf of 200 Hz. The antenna system essentially produces a time-derivative of the input pulse in the far field.

Pulser Design

The oil-air lens diameter of ~ 25 cm and the $\gtrsim$ 15 cm transmission line conductor spacing that results at the lens were chosen to avoid breakdown in air at up to 150 kV (average electric field < 10 kV/cm). The lens consists of a volume of oil inside a container of polypropylene (chosen because its permittivity of 2.3-2.4 is close to that of oil) that is machined to the desired lens shape. The lens design chosen is one of a continuous set in which the rays emerging from the oil bend towards the dish axis as in the actual lens, Figure 2(a)[1], or away from the dish axis, Figure 2(c). The special case of a spherical lens and no bend, Figure 2(b), lies in between; it has the disadvantage that rays are internally reflected from the interface exactly towards the oil apex, and will have more tendency to be re-reflected back towards the dish with no

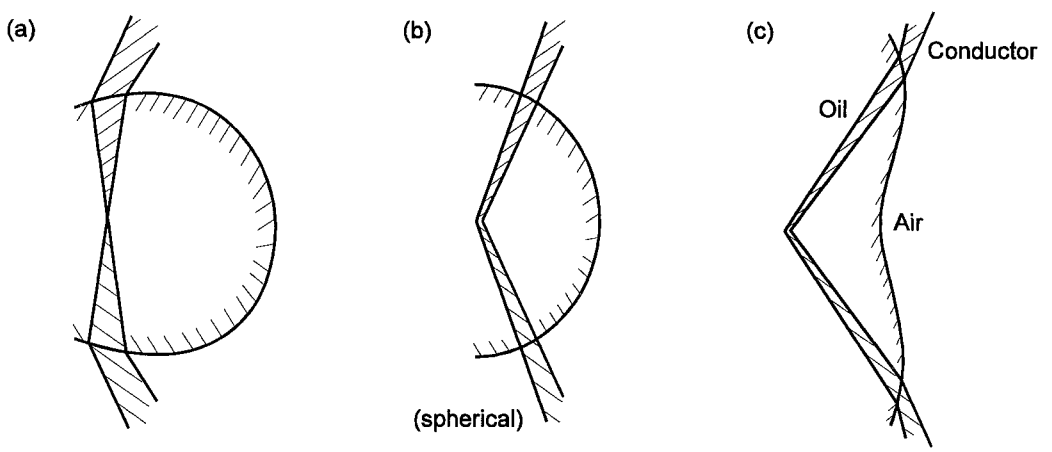

Figure 2. Schematics of possible lens designs.

dispersion, perturbing the waveforms and spectrum more. A design like Figure 2(c) was explored early in the program because it minimizes the thickness of plastic from which the lens is machined. The chosen design has the advantage that in the oil the midlines of the conductors lie in the vertical plane, greatly simplifying the mechanical design.

Ideally, the conductors in oil should comprise four thin triangular plates, forming a 133-ohm transmission line, that taper to very small dimensions near the system axis; this would minimize the size of the region near the axis where the pulse is launched on the line, and so help its risetime be minimized. Distortions of this ideal line geometry are necessary to accommodate the capacitors and switch, and these distortions must be minimized. Thus the four capacitors have trapezoidal sections that closely match a portion of the line and have thicknesses of only 1 cm. The 3.8 cm capacitor length in the direction of the line conductors gives a charging field of about 20 kV/cm. The required 0.1 nF capacitance for each capacitor (and for four in series parallel) is obtained by using a ceramic with a permittivity of over 3000. Because of this high permittivity, the wave will, to first order, sweep over the capacitor surface as over a metal. To second order, the wave is expected to develop a voltage across the capacitor proportional to the wave impedance of its faces; this impedance should be intermediate between the values of 14 ohms and 7 ohms, which

correspond to one and two large faces; taking a value of 10 ohms and dividing it by twice the 133-ohm line impedance, 3-4% of the wave voltage will be developed on the capacitor. It is this wave, constantly reflecting inside the capacitor, that eventually discharges it.

Though we have discussed a "voltage" developed at the capacitor, any effect of the capacitors on the radiated field will vary with direction, being seen more quickly for rays passing close to the capacitors and later for rays in between, including near the axis. Though design considerations suggested their effect everywhere would be small, the capacitors were placed as close to the lens surface as possible and thus as far as possible from the switch, to delay any such effects, certainly till somewhat after the end of the risetime for positions on-axis.

The capacitors are held in place in the transmission line by plastic clamps that compress them between conductors whose cross-sections match the capacitor ends, with conductive epoxy ensuring good contact. The conductors that join the capacitors to the switch taper in all dimensions in proportion to distance from the system axis, Figure 3. The switch itself is cylindrical, with two circular endplates. To each of these end-plates the two line conductors of the same charge polarity connect as a single unit, the "wingnut" conductor in Figure 3.

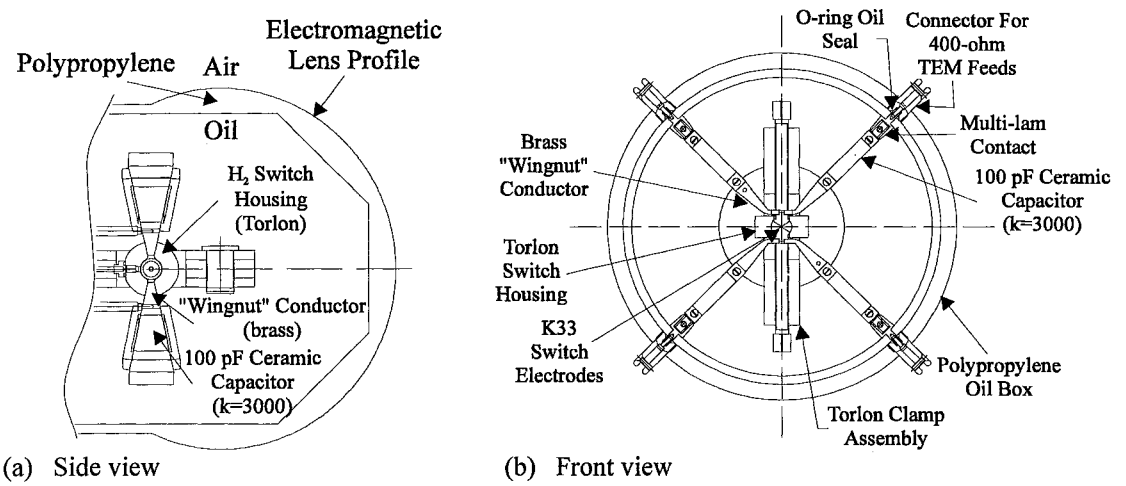

Figure 3. Pulser oil volume showing lens.

The choice of switch medium is determined by the fast risetime and the repetitive operation needed. At voltages of a few hundred kV and below, the calculated risetimes of gas switches are dominated by the resistive phase, according to J.C. Martin's expression: τ_r (10-90%) ~ 8.5 $\rho^{1/2}$ / $E^{4/3}$ $Z^{1/3}$ nsec . Here Z is the impedance being driven, which is fixed and it appears necessary to minimize $\rho^{1/2}/E^{4/3}$, where ρ is the gas density (g/cc) and E the switching field (MV/cm). Because the E-dependence of τ_r is much stronger than the ρ dependence, high pressure is indicated. At room temperature, SF_6 liquefies at ~ 20 bar with τ_r ~ 1 nsec. Air and hydrogen can both be used at much higher pressure giving τ_r << 1 nsec. Hydrogen should be better, since at the same pressure $\rho^{1/2}$ is only ~ 0.25 times that of air while E is in the range 0.6 - 0.7 of that of air, so that $E^{4/3}$ is less by about a factor of two. Hydrogen also has the potential of achieving >1 kHz operation without the need to flow the gas fast enough to move the arc products far from the high field region between pulses[2].

Recently, oil has also been used by Morton et al. at PSI, in extensions of Reference 3, to achieve 0.1 nsec risetime at > 600 kV, and > 1 kHz at a power-supply limited voltage of ~ 300 kV. However, this requires high speed oil flow through the switch. Also, obtaining the fast risetime requires charging in nanoseconds to reach a breakdown field of ~ 5 MV/cm, and this would require the use of a more complex peaking circuit.

In the case of hydrogen, data obtained from Sandia indicated that the breakdown strength was a very weak fraction of charge time from nanoseconds to microseconds. A charge time of hundreds of nsec was selected as the fastest that could be obtained without heavy demands to make the charging transformer and the connections to the pulser (the umbilical, see below) very low inductance.

The switch is shown in more detail in Figure 4. It has cylindrical symmetry to ease the mechanical design for very high pressure. The plastic pressure vessel is of Torlon, and is ~ 1.5 cm high. Hydrogen is fed in through a hole in the midplane of this vessel. The metal electrode endplates with O-ring seals are held in place by a Torlon clamp assembly. The metal electrodes in the gas form a biconic region whose impedance (~ 80-ohms) is made smaller than the 133-ohms of the oil transmission line in order to increase the current density towards the value that needs to be delivered to the transmission line conductors where they attach to the endplates. The tips of the two cones are of tungsten copper alloy, and their spacing of about 1 mm can be adjusted with shims.

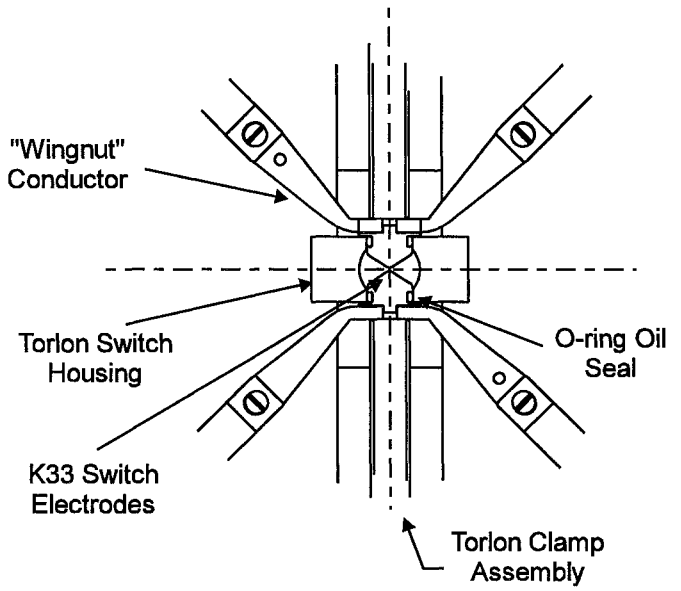

Figure 4.

The capacitors are charged by a modulator consisting of a 1 kJ/sec, 30 kV power supply, an EEV CX1551 thyratron, and a Stangenes Industries pulse transformer with a 7:1 gain and a differential output. The modulator is located behind the dish, and is connected to the oil pulseforming region by the high voltage umbilical feed, which lies in the symmetry plane of the transmission lines where the E-fields parallel to the plane are zero. This feed is a twisted pair of No. 12 AWG silicone rubber insulated wires spaced 5 cm apart in a 7.6 cm diameter clear plastic tube at up to 10 psig of SF_6. The insulation scheme minimizes capacitance, and the twisting minimizes coupling to the wave. The voltage at the input to the feed is monitored by two resistive dividers. The feed tube also encloses pipes that bring flowing oil to the pulser to cool its components, and hydrogen gas to the switch. Total hydrogen volume, including the feed, is < 5 cm^3. The high voltage feed transmission line is decoupled from the hydrogen switch by resistors and inductors located in the oil on the side of the switch away from the dish. The plus/minus charging current from the feed to the capacitors flows to ground through the transmission line, termination resistors, and dish.

If the hydrogen spark gap operates at ~ 125 kV with 1 mm gap at 100 atm., the resistive phase formula given above indicates a risetime of about 100 ps driving the 133-ohm oil line. The channel inductance of about 1 nH contributes less than 20 ps. The other risetime contribution expected is that of the mismatch between geometries of the bicone switch and the four-conductor line in oil. We might estimate this from

resistive phase of the hydrogen switch may be less than predicted; this is not surprising, because the resistive phase formula was derived for different gases and electric fields.

The pulser performance envelope is illustrated in Figure 8. Its capabilities were limited by the power supply and modulator whose capabilities were budget-limited. It is believed that a simple upgrade of the power supply and modulator would allow operation at 1-2 kHz.

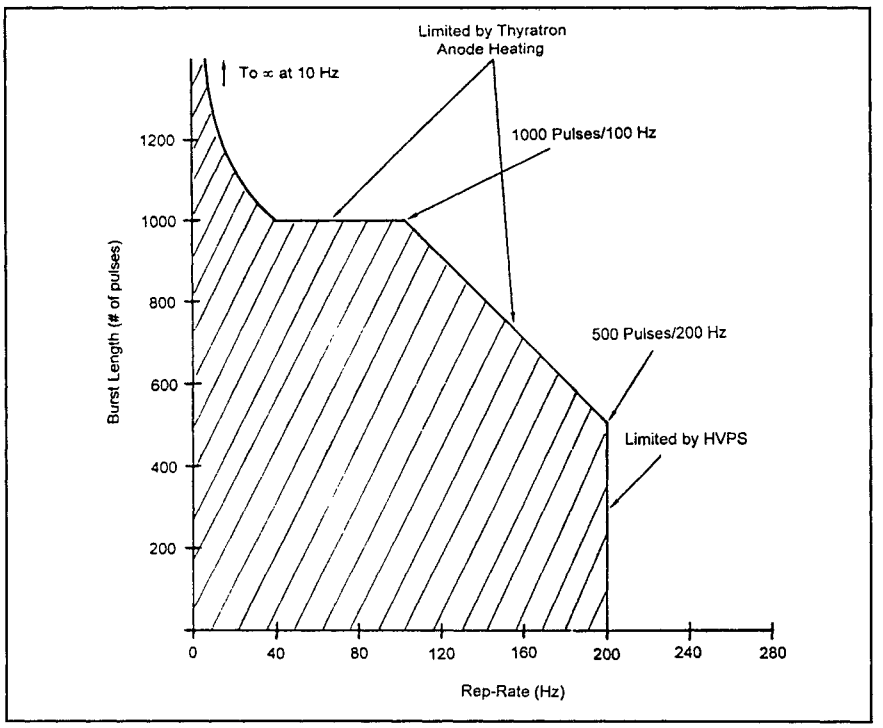

Figure 8. Pulser performance envelope (28 kV charge ≃ 130 kV out).

Moreover, the basic pulser-lens unit should be capable of operation at significantly higher voltage. Capacitor materials are available that should operate at 50 kV/cm rather than 20 kV/cm, so that the same configuration could be charged to ~ 300 kV. Addition of an atmospheric SF_6 gas region to a radius of about 40 cm would probably avoid breakdown outside the lens at that voltage. For that level the present switch could be scaled up by a factor of two with some increase in pressure (to ~ 150 bars). A slightly longer risetime would be expected, partly because of the geometric risetime term; however, alternative switch geometries have been identified that better match the four-conductor line geometry. These were judged impractical to construct on the same of the present switch but they could be used on the larger scale with some advantage. Thus a modification within the present lens volume may give $\lesssim$ 100 ps risetime at ~ 300 kV

Antenna Performance

The reflector IRA that has been fabricated and tested is shown in Figure 9. It consists of a solid-surface, spun-aluminum, paraboloidal reflector of diameter D = 3.66 meters and focal length F = 1.21 meters. The antenna is fed by two mutually orthogonal co-planar conical lines diverging in air as if from the focus. Each line has a TEM characteristic impedance of 400-ohms giving a net impedance of 200-ohms. The terminating impedances (200-ohm dc and some capacitance) connect the end of the four plates to the dish near its edge. These impedances were experimentally optimized using a TDR measurement that employed a TEK-109 (50 V, 180 ps rise) pulse.

the capacitance of the cone, about 0.4 nF including the fringing capacitance in oil and plastic; if this is charged by the bicone and the oil line in parallel (~ 50 ohms), the 10-90 charging time is of the order of 50 ps. Neither this nor the inductive risetime would be expected to add significantly to the 100 ps resistive phase component.

Pulser Performance

The pulser risetime was best measured by an MGL-7 B-dot sensor placed at the center of the dish to record the arrival of the wave launched by the pulser. Figure 5 shows the raw and software-integrated waveforms recorded on a TDS-820 sampling scope during a 512 pulse, 200 Hz burst at about 120 kV on the switch. The 10-90 risetime of the integrated pulse is typically 130 ps (± a few ps) in such runs. The MGL-7 is believed to have a 100 ps risetime, the TDS-820 has a specified risetime of 58 ps, and the cables totaling 2-ft. that connect them had a risetime measured approximately as 63 ps; added in quadrature these total 130 ps, so the indication is only that the pulser risetime is less than this, perhaps significantly less. Note that no feature can be identified on the waveform that is the result of the capacitors, which should be "seen" at 150-200 ps after the start of the rise.

An MGL waveform measured over a 20 nsec is shown in Figure 6. During the initial 1.4 nsec the output voltage is increased by a 1.2 transmission coefficient from oil to air; the reflection from the lens and the switch that ends this enhanced voltage is clearly seen. After 6 nsec more of fairly smooth decay, the region where the resistors connect the transmission lines to the dish is seen at the MGL-7 at the dish center, and shortly afterwards the edge of the dish is seen. Until the termination is seen, the magnetic field at the conducting dish is double that in the propagating wave. The signal from the termination thus reduces the field. The finite size of the dish concentrates the current at the center, however. These the waveform details are not yet understood quantitatively, but the amplitude soon returns to near what it was just before 6 nsec, and then continues to decay. Overall, the decay fits the expected 20 nsec e-fold.

Figure 7 shows the plus and minus charge voltage in a full-voltage, 200 Hz burst, recorded in envelope mode. It is seen that the reproducibility of self-breakdown of the hydrogen switch is quite good, the total spread in the 512 pulse burst being only about 10%. As expected, no reduction in self-break voltage was noticed at 200 Hz. The total charge voltage, which is recorded at the input to the umbilical feed, is 125 kV in Figure F; circuit simulations predict that the switch voltage will be slightly lower, about 115 kV. The voltage transmitted through the oil-air mismatch should be V ~ 135 kV. This should generate ~ 40 kV/m incident on the dish; the MGL-7 indicates 34 kV/m, which corresponds to V ~ 115 kV.

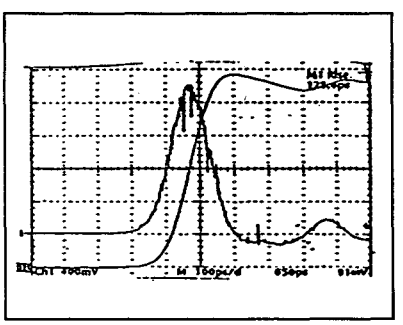

Figure 5. Current density at dish on-axis (129 ps rise).

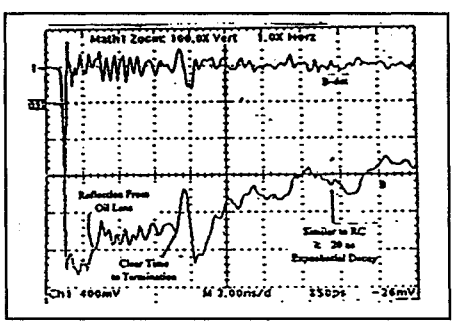

Figure 6. Current density at dish on-axis for first 19 nsec.

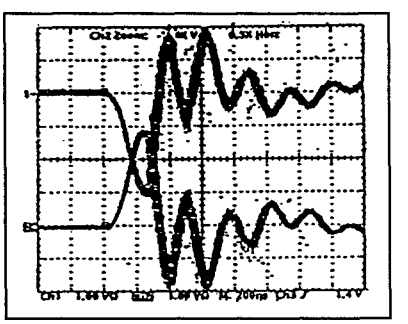

Figure 7. Voltages at input of feed line, 200 ns/div (± 63 kV peak).

In summary, the pulser performance was 115-135 kV, ≲ 100 ps 10-90% rise, 20 nsec e-fold decay, 200 Hz; these results easily met the project goals of > 100 kV, < 150 ps, > 15 nsec and > 100 Hz. The

The analysis of this prototype IRA in terms of its radiated field along its optical axis was performed (SSN 365, Reference 4) and the result is shown in Figure 10. This analysis assumes an ideal step function input, while the practical pulser is a fast-rising (~ 100 ps), slowly-decaying, double exponential.

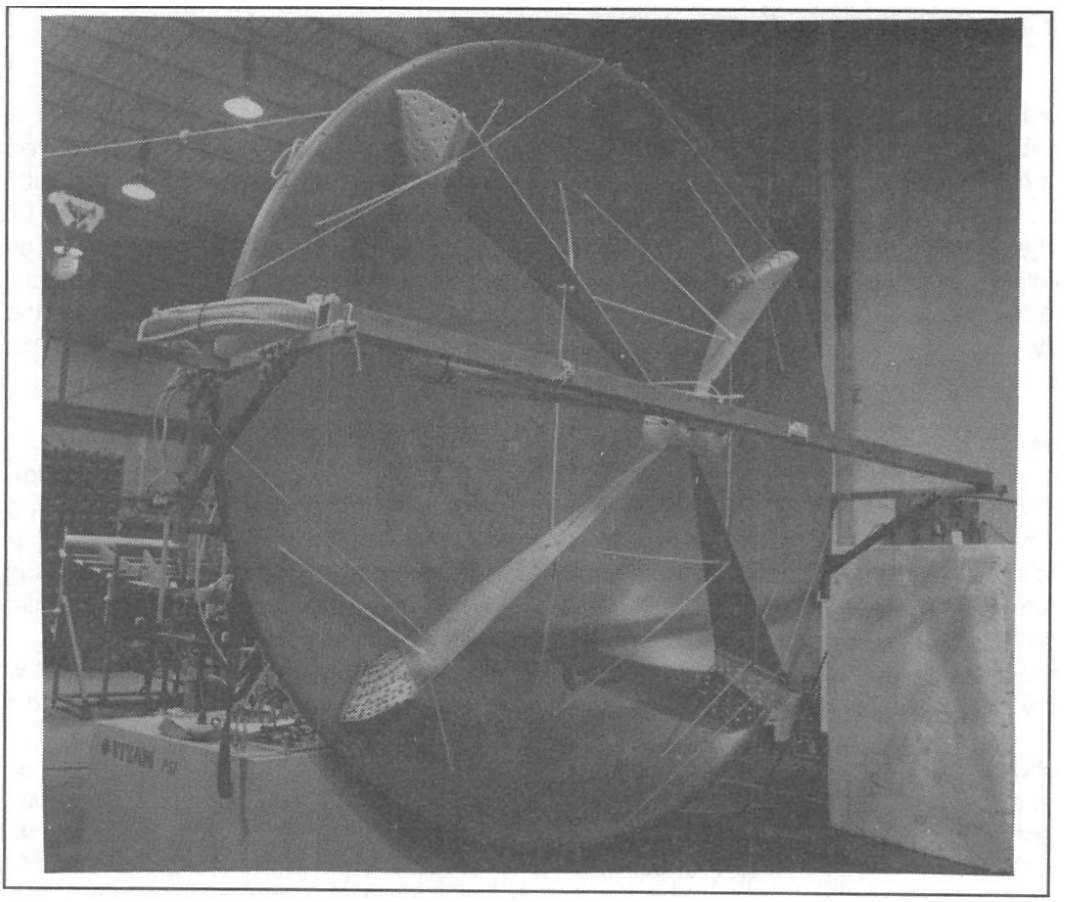

Figure 9. Prototype reflector IRA.

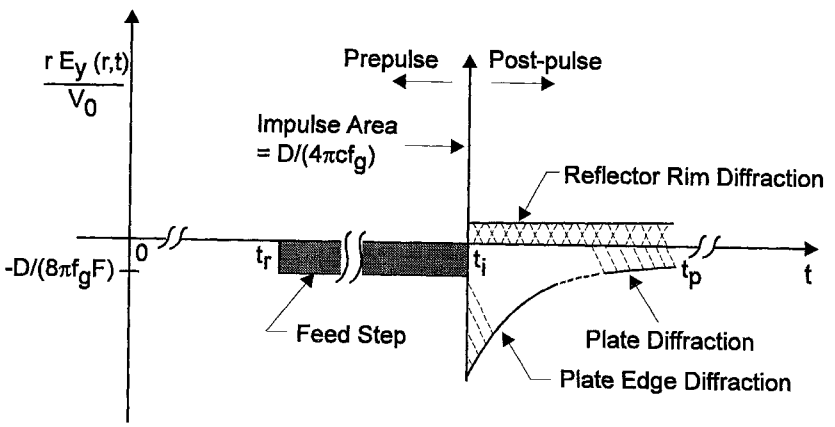

$$(t_r = r/c\,,\ t_i = t_r + (2F/c)\,,\ t_p = t_i + (b/c)$$

Figure 10. On-axis radiation from a canonical reflector IRA of Figure 1, when it is fed by an ideal step function pulser.

The performance quantities of interest are the near and far fields. Near fields (~ 34 kV/m at the center of the reflector) have been discussed earlier and we will now focus on the far field measurement. One then is faced with the question of, where does the far field with its (1/r) dependence begin? In time-domain applications, we require

$$\frac{\Delta r}{c} < t_{10-90}\ (rise)$$

where Δr = differential travel distance to the observer from the center and edge of the reflector. For the present case r = 300 meters leads to $(\Delta r/c) \simeq 19$ ps which is about 20% of the risetime. Our far field measurement was performed at r = 304 meters on the optical axis of the antenna. A sample measurement of the radiated field at a distance of r = 304 meters is shown in Figure 11. The azimuthal variation of the peak electric field is shown in Figure 12. From this measurement, we observe that

$$V_{far} = r\,E_{far}\,(peak) \cong 1281\ kV$$

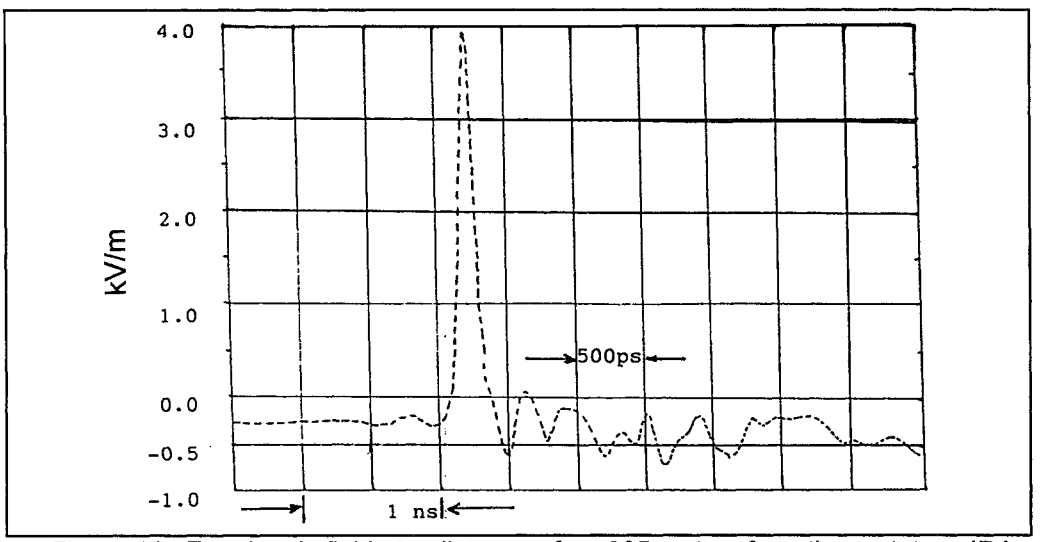

Figure 11. Far electric field at a distance of r = 305 meters from the prototype IRA.

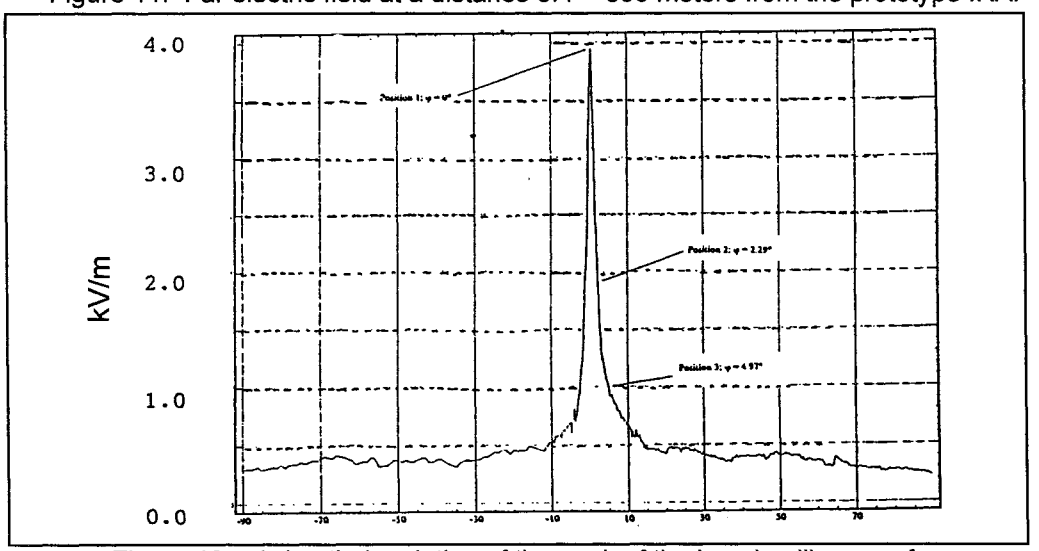

Figure 12. Azimuthal variation of the peak of the impulse-like waveform.

Measured (V_{far} / V_{plates}) > 10, is indicative of the impulse-like behavior of the far field. The radiated field is also seen to have a FWHM ≃ 130 ps, resulting in an extremely wide bandwidth. The measured performance of the antenna is summarized in Table 1. The far field of Figure 11, displays the negative feed step, which is the direct radiation from the hydrogen switch (≡ source), followed by the narrow impulse. This impulse-like field has a nearly flat spectrum extending from about 50 MHz to about 2.5 GHz. The limitation at the lower end of frequencies is governed by the antenna size, while the high-frequency roll-off in the radiated spectrum is related to the risetime of the input pulse. This resultant wide spectrum of the radiated field of the prototype IRA system described here, is expected to lead to many applications in areas such as hostile target identification, buried object detection, high-power jamming, etc.

Table 1. Summary of the reflector IRA measurements.

Physical Quantity	Numerical Value
Peak Electric Field on Boresight at r = 305 meters	4.2 kV/m
Boresight Electric Field (10-90%) risetime, r = 305 meters	99 ps
Boresight Impulse Duration (FWHM), r = 305 meters	130 ps
Boresight Electric Field Spectrum, r = 305 meters	< 12 db variation over 50 MHz - 4 GHz
Main Beam Scan: FWHM θ - beam width FWHM ϕ - beam width	 -1.77°, +1.45° -0.98°, +2.31°
Azimuthal or H-plane Pattern FWHM ϕ - beam width -3 dB peak power beam width	 3.18° 1.80°
Incident Electric Field at the Center of the Dish (10-90%) Risetime	~ 34 kV/m 126 ps*
$V_{far} = r E_{far}$	~ 1281 kV
*(instrumentation limited sensor ~ 100 ps, scope ~ 56 ps)	

References

1. C.E. Baum, J.J. Sadler, and A.P. Stone, *"A Uniform Dielectric for Launching A Spherical Wave Into A Paraboloidal Reflector,"* Sensor and Simulation Note 360, 22 July 1993.

2. M. Grothaus, et al., *"Recovery Characteristics of Hydrogen Spark Gap Switches,"* Proc. IEEE Pulse Power Conference, 1993.

3. P. D'A. Champney, et al., *"The Development and Testing of Subnanosecond-Rise, Kilohertz Oil Switches,"* Proc. of 8th IEEE Pulse Power Conference, June 16-19, 1991.

4. D.V. Giri, Protech and C.E. Baum, Philips Lab., *"Reflector IRA Design and Boresight Temporal Waveforms,"* Sensor and Simulation Note 365, 2 February 1994.